

Monitoring Ground Settlement in Hong Kong with Satellite SAR Interferometry

G.X. LIU, Y.Q. CHEN, X.L. DING, Z.L. LI, and Z.W. LI, China

Key words: Synthetic aperture radar (SAR), interferometry, ground settlement.

ABSTRACT

Due to the scarcity of useable land in Hong Kong, it is a common practice to reclaim land from the sea. The reclaimed land usually undergoes a long period of settlement that may affect building structures and underground facilities such as water supply and sewage systems built on the land. Measurements of land settlement can provide valuable data for assessing the impacts of land settlement and for improving designs of future land reclamation projects.

Research has been conducted to use satellite synthetic aperture radar interferometry (InSAR) to monitor ground settlement of some reclaimed land areas in Hong Kong. This paper examines the sensitivity of the technology in such applications, addresses the data processing issues and limiting factors of the technology, and presents some initial test results obtained with the repeat pass ERS-1/2 satellite radar images, including settlement measurement results over the new Check Lap Kok Airport that was built on reclaimed land.

CONTACT

Dr. Xiaoli Ding, Associate Professor
Department of Land Surveying and Geo-Informatics
Hong Kong Polytechnic University
Hung Hom, KLN
HONG KONG, CHINA
Tel. + 852 2766 5965
Fax + 852 2330 2994
E-mail: lsxlding@polyu.edu.hk
Web site: <http://www.polyu.edu.hk>

Monitoring Ground Settlement in Hong Kong with Satellite SAR Interferometry

G.X. LIU, Prof. Y.Q. CHEN, Dr. X.L. DING, Dr. Z.L. LI, and Z.W. LI, China

1. INTRODUCTION

It is a common practice to reclaim land from the sea in Hong Kong (HK) due to the scarcity of useable land in the territory. Reclaimed land usually undergoes long periods of settlement that may affect building structures and underground facilities such as water supply and sewage systems built on the land. Monitoring of the progressive settlement of reclaimed land can provide valuable information to assess the impacts of land settlement and to improve future designs of land reclamation projects. There are many different methods available for monitoring land settlements, although they can generally be grouped into two categories, geodetic and geotechnical techniques (Ding et al., 2000). Almost all of the existing techniques rely on collection of data repeatedly at selected points, and then derive the magnitudes and rates of settlement from measurements obtained at different epochs. These point-based measurement methods are generally expensive and inefficient for monitoring large settlement areas. Besides, sparsely distributed data points are often difficult to provide information on very localised land settlement.

Satellite synthetic aperture radar interferometry (InSAR) has recently been demonstrated to be a promising tool for mapping ground deformations without the need of laborious field accesses. InSAR uses multiple SAR images acquired at different times over the same region to infer ground displacements of the region. InSAR is an area-based measurement technique that offers much higher spatial resolution (decametres), good spatial coverage (thousands of square kilometres), and very competitive accuracy (millimetres to centimetres) under good conditions. In addition, InSAR works day and night and under all-weather conditions, and is highly automatic in data processing. The special characteristics of InSAR make it a convenient, efficient and economical tool to study many geophysical and geodynamics problems. The main disadvantages of the current InSAR technology include its high sensitivity to atmospheric conditions, unsuitability or difficulty in measuring steep ground surfaces and areas covered with heavy vegetations, and that it only measures displacement along the radar line of sight (LOS) direction (e.g., Liu and Ding et al., 2001a).

InSAR has been applied to measure ground settlement related to, for example, the shrinking/swelling of irrigated fields (Gabriel et al., 1989), geothermal power production (Massonnet et al., 1997), aquifer system compaction (Galloway et al., 1998), underground quarries (Fruneau et al., 2000), and ground water pumping (Bawden et al., 2001). Usually ground settlement is a rather slow process and requires a long time period (e.g. months to years) of accumulation to be significant enough for InSAR to detect. Longer time intervals between the acquisitions of SAR images however generally mean lower radar coherence between the images, hence less reliable subsidence measurements. In addition, atmospheric effects can often become significant when settlement over a long time period is measured with InSAR (e.g., Zebker et al., 1997).

This research will employ some ERS-1/2 satellite radar images to study the land settlement problems in HK. In particular, we will examine the sensitivity of the technique in such applications for the field environments and atmospheric conditions in HK, and addresses the data processing issues and limiting factors for the applications. Test results for selected areas in HK including the newly constructed HK Airport will be presented.

2. INSAR METHODOLOGY AND ITS SENSITIVITY TO GROUND SETTLEMENT

Study of ground deformation with InSAR begins with the generation of interferograms by differencing the phase values of two co-registered radar images acquired at different times over the same target area. Direct phase difference at each pixel is related to the range change in the radar LOS direction between the two satellite passes. The observed phases contain information on: (1) the nonzero flat-earth phase trend and natural topography in the case of nonzero-baseline interferometry, (2) surface movements/deformations between the two image acquisitions (e.g., Liu and Ding et al., 2001b), (3) possible path delays due to temporal-spatial atmospheric inhomogeneity (e.g., Zebker et al., 1997), (4) random noise, and (5) biases in data processing. The unwanted noise may be due to temporal decorrelation resulted from disturbance of radar-backscattering surface (e.g., leaf fluttering, growth of vegetation and changes in land cover), baseline decorrelation resulted from different cross-track sensor positions, and thermal noise of the SAR sensor (e.g., Zebker et al. 1994b). The signal to noise ratio in an interferogram can be measured to some extent by the associated coherence map (i.e., signal correlation coefficients) (e.g., Rosen et al., 1996).

The temporal decorrelation and atmospheric effects are two main uncontrollable limiting factors in InSAR applications (e.g., Rosen et al., 1996; Zebker et al., 1997; Chen et al., 2000). Generally, atmospheric effects and random noise are expected to be insignificant and thus acceptable in an interferogram. In the absence of ground movements, an interferogram can be used to map the topography (e.g., Zebker et al., 1986, 1994b). Otherwise, the interferogram can be used to detect ground deformations when the flat-earth phase trend and topographic effects in the initial interferogram are removed. The latter is referred to as differential interferometry processing (DIP) and it generates the so-called residual interferogram. There mainly exist two DIP approaches, i.e., the two-pass method proposed by Massonnet et al. (1993) and the three-pass method after Zebker et al. (1994a).

It is important to realise that the phase value at each pixel in a differential interferogram is ambiguous to within the integer multiples of 2π , and that the phase in an absolute sense needs determined by the so-called phase unwrapping algorithms (e.g., Goldstein, 1988). The derived absolute phase values (ψ_m) is converted to the LOS range change (ΔR) by,

$$\Delta R = \frac{\lambda}{4\pi} \cdot \psi_m \quad (1)$$

where λ is the radar wavelength. In the absence of horizontal movement, vertical movement Δh can then be calculated with

$$\Delta h = \frac{\Delta R}{\cos \theta} = \frac{\lambda \cdot \psi_m}{4\pi \cdot \cos \theta} \quad (2)$$

where θ is the local radar incident angle.

In the case of ERS-1/2 C band ($\lambda=5.6\text{cm}$) SAR system (nominally $\theta=23^\circ$), it is readily derived by equation (2) that the sensitivity of phase to subsidence is about 3.0cm, i.e., one full phase cycle (2π) can detect 3.0cm vertical change. However, as for JERS-1 L band ($\lambda=23.5\text{cm}$) SAR system (nominally $\theta=35^\circ$), the corresponding sensitivity value is 14.3cm. Given a phase rms error of 40° , the subsidence error is 3.0mm for the case of ERS-1/2 images, and 15.9mm for the JERS-1 images. It is clear from the analysis that the longer the radar wavelength is, the less sensitive the system is to ground subsidence. On the other hand, long wavelength data are more robust in terms of maintaining temporal correlation over vegetated areas (e.g., Rosen et al., 1996). Since most of the reclaimed land in HK is not heavily vegetated, the ERS interferometer is more preferable for the measurement of land settlement.

Past analysis has shown that the suitability of an interferometric pair for observing the Earth mainly depends on their orbital separation, or more specifically, on the length of baseline component perpendicular to the radar LOS (sometimes termed as effective baseline). Topography mapping requires moderate perpendicular baseline (e.g., 150-300m for ERS-1/2 case) to balance between the sensitivity of the phase to elevation variations and baseline decorrelation (Massonnet et al., 1998), whilst settlement detection demands the baseline to be as short as possible (Zebker et al., 1994a).

For land settlement measurement in this study, we employ the two-pass DIP approach and use orbital data and an existing digital elevation model (DEM) to remove the flat-earth trend and the topographic contributions (Massonnet et al., 1993). However, the error (δh) in the DEM can propagate into the differential interferogram and cause the following phase error:

$$\delta\phi = \frac{4\pi}{\lambda} \cdot \frac{B_\perp}{R \cdot \sin \theta} \cdot \delta h \quad (3)$$

where R is the slant range from the satellite to the ground and B_\perp is the length of effective baseline. $\delta\phi$ approaches 0 when B approaches 0. Therefore a short baseline can limit the propagation of DEM errors.

3. STUDY AREAS AND INSAR DATA SETS

Two reclaimed land areas in HK, the newly built Chek Lap Kok Airport (approximately 10km^2) and a residential area Fairview Park (approximately 2km^2) (Figure 1b) are chosen for the study. We will mainly focus on the former, discussing the data processing and analysis involved and the results, while will only give the results for the latter.

The Chek Lap Kok Airport started its operation on July 6, 1998, to replace the old Kai Tak Airport that had served HK for 73 years. The new airport was built over a large man-made island of 12.48km^2 , north of the Lantau island (see Figure 1b). Three-quarters (9.38km^2) of the land used for the airport was reclaimed from the sea, whereas the remaining quarter was formed by excavating two existing granitic islands, the Chek Lap Kok island (3.02km^2) and the Lam Chau island (0.08km^2), as highlighted in Figure 1c and Plate 1 (Plant et al., 1998). The site reclamation that involved dredging of unsuitable material (marine mud) and placement of fill materials (rock and sand) was carried out from December 1992 to June 1995. Although the most compressible marine mud had been largely removed, the reclaimed

land is still subject to settlement. This stems from compression of both the fill materials and the soils beneath the seabed. Since the opening of the airport, the stability of the airport platform has been routinely monitored by levelling measurements by the Airport Authority (see Plate 1).

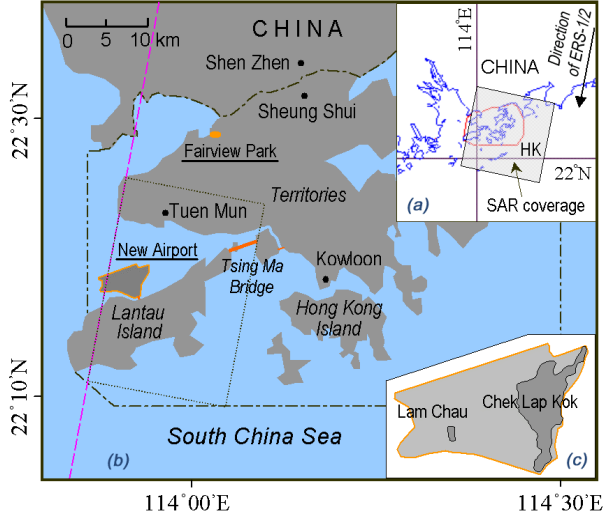


Figure 1. (a) Full coverage of ERS SAR scene over HK; (b) Location map of the study areas (the Airport and Fairview Park) with the box showing the area of interferograms given in Plate 2; and (c) Enlarged view of the airport platform (after Plant et al., 1998).

Five ERS-1/2 SAR images acquired over HK during 1996-1999 are used for this study. All the images were acquired at around 10:54am local time (frame 3159 in track 404) along a descending orbit (travelling north to south and looking to west). Figure 1a shows the coverage of the SAR scene and the satellite flight direction (azimuth 191.8°). Unfortunately, a very small portion in the west part of the new airport was not covered by the image as shown in Figure 1b.

Among ten possible interferometric combinations of the five images, only 3 pairs (03/18-03/19, 1996, a Tandem pair; 11/24-12/29, 1998 and 12/29/1998-11/09/1999) maintain enough coherence for the airport area. The actual interferogram formation will be restricted to the area of interest (about 25 km in azimuth by 17 km in ground range) that is marked by the rectangle shown in Figure 1b. An enlarged SAR amplitude image of the airport is shown in Plate 1, on which the positions of the 28 benchmarks used for later analysis are plotted.

4. DATA PROCESSING AND INTERFEROMETRIC RESULTS

To obtain a differential interferogram across the airport, our interferometric data processing chain includes: (1) accurately co-registering two SAR images, (2) forming and filtering an interferogram, (3) removing flat-earth trend phases using precise orbit data, (4) removing topographic phases using independent DEM, and (5) phase unwrapping. The DEM used is created from the digital map provided by the Lands Department of the HK Government. The

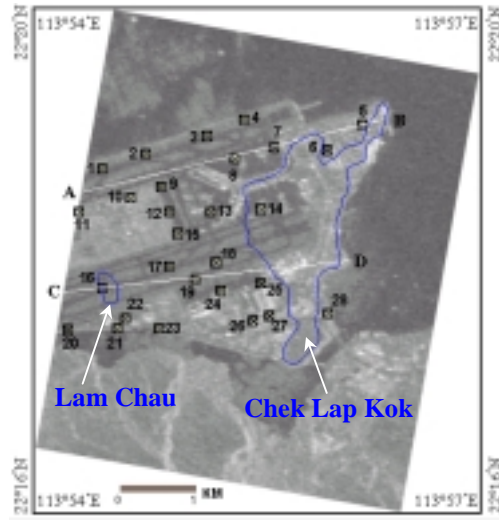


Plate 1. SAR amplitude image across the airport. The numbered points are benchmarks plotted over the image. The original outlines of the two excavated islands are also plotted. Lines AB and CD are drawn as reference for Figure 3.

rms error of the DEM is smaller than 1.0m. The phase unwrapping is carried out with the branch-cut method (Goldstein et al., 1988), starting at the pixel corresponding to benchmark No. 14 (see Plate 1) and assuming its phase value equal zero.

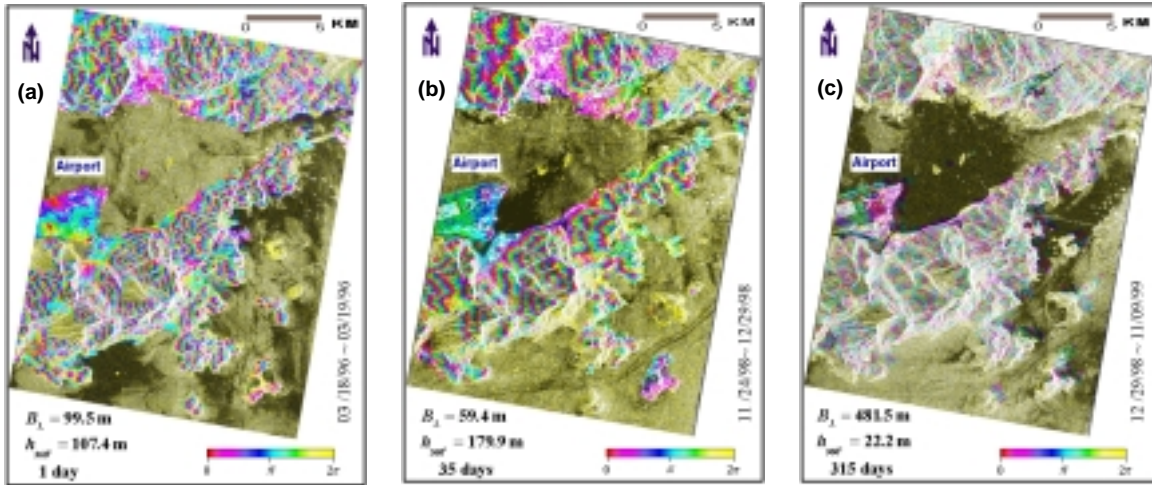


Plate 2: Interferograms of the study area with different time intervals. Radar amplitude images and coherence maps are superimposed on the interferograms. After removing flat-earth trend phases, the remaining interferometric phases or “fringes” are due to the topography, possible ground settlement, random noise and/or atmospheric effects.

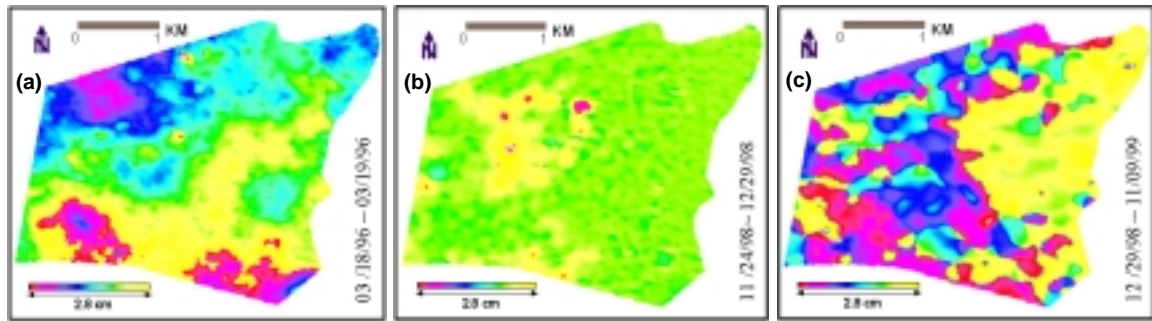


Plate 3: Enlarged view of the differential interferograms of the study area. One cycle of interferometric phase change (see the colour scales) represents half wavelength (28mm) range change in the LOS direction.

4.1 Interferograms

Plate 2 shows three interferograms in the Universal Transverse Mercator (UTM) projection after removing the flat-earth trend phases. The radar amplitude images and coherence maps are superimposed on the corresponding interferograms to show the interferometric quality. The interferometric parameters (effective baseline, ambiguity elevation and time interval) are shown in the bottom-left corner of each interferogram. Fringes in Plate 2 are resulted from contributions of the topography, possible settlement, random noise and/or atmospheric delays. To reduce the phase noise, each interferogram was filtered by a multi-looking or pixel averaging operation (1 look in range by 5 looks in azimuth), resulting in a resolution of 20 m by 20 m. The fringeless areas shown are those where phase measurements are too noisy or

where it is the sea. The observed fringe rates are different between the three interferograms. The larger the effective baseline is, the higher the fringe rate would be. The 315-day interferogram (Plate 2c) has the highest fringe rate; the 1-day interferogram (Plate 2a) has a moderate fringe rate, while the 35-day interferogram (Plate 2b) has the lowest fringe rate. Besides, the fringes in the short-term interferograms (1 day and 35 days) are much clearer than those in the long-term one (315 days), especially over the vegetated areas such as on the Lantau Island, due to temporal decorrelation. The airport area maintained good coherence (>0.38 in average) in all interferograms.

Differential interferograms are then generated by using the two-pass DIP method to remove the topographic phase term from the interferograms shown in Plate 2. The results over the airport are shown in Plate 3, where each residual fringe corresponds to LOS range change of half a radar wavelength (28mm). Since the flat-earth trend phase and the topographic phase have been removed, the residual phase can be considered to be the radar range changes caused by uneven ground settlement, atmospheric effects and random noise.

At the first glance, the three differential interferograms present noticeable different features. Plate 3c shows significant differential phase variations that are most likely resulted from ground settlement accumulated over the 315 days. It is very interesting to note that the measured phase values appear to be very smooth across the two excavated islands, Chek Lap Kok and Lam Chau, indicating no or little ground settlement in the areas since they consist of original stable granite (Plant, 1998). Over the reclaimed areas however, the phase values vary significantly, even over one day period where phase variations of nearly two fringes are visible (Plate 3a). The most likely reason for the fringes in the one-day interferogram is atmospheric delays since it is unlikely to have such significant settlement over the short time period.

4.2 Atmospheric effects and error analysis

There are four possible error sources that could limit the accuracy of the settlement measurements, i.e., (1) errors in the orbital parameters, (2) errors in the DEM, (3) phase noise caused by radar decorrelation, and (4) possible atmospheric effects. The orbital errors are negligible as the study area is small (Zebker et al., 1994b). According to equations (2) and (3), 1.0m error in the DEM can lead to 0.2mm (35-day pair) to 1.0mm (350-day pair) errors in the measured settlement. The errors are therefore considered insignificant since the accuracy of the DEM is better than 1m. Error sources (3) and (4) are assessed below.

The phase standard deviation (SD) δ_ϕ is first estimated statistically, and then theoretically by using the Cramer-Rao bound formula:

$$\delta_\phi = \frac{\sqrt{1-\gamma^2}}{\gamma \cdot \sqrt{2N}} \quad (4) \text{ where } \gamma \text{ is the coherence level, } N \text{ is}$$

the window size of the multi-looking operation (5 in this case). Comparison will be made finally between the statistical and the theoretical results.

The excavated island (about 3km²), Chek Lap Kok (see Plate 1) is more stable as discussed earlier and is used as the sample area. The area contains 6686 pixels and has an average coherence level of 0.68 (one-day), 0.52 (35-day) and 0.35 (315-day), respectively. Figure 2

shows the comparison between the statistical and the theoretical SD estimated for the three interferometric cases. The values for the one-day interferogram (0.3rad and 2.2rad respectively) are most inconsistent, whereas very good agreements exist for the 35-day (about 0.6rad) and 315-day (about 0.85rad) cases. The same calculations have also been done for the small Chau Lam island ($400\text{ m} \times 200\text{ m}$) to study the possible spatial variations of the results. Very similar results are obtained, indicating the spatial variations are insignificant.

It can be seen from the above analysis that the fringes that appear in the one-day interferogram are most likely caused by the varying atmospheric inhomogeneity, while the other two interferograms were hardly contaminated by atmospheric effects. Figure 3 shows the atmospheric effects in the one-day interferometric pair, along the north (Figure 3a) and south (Figure 3b) runways. The two profiles indicate significant (4cm) phase variations. As illustrated by the curves fitted to the results, the atmospheric phase changes have a wavelength of longer than 4 km.

The random noise in an interferogram resulted from radar decorrelation is a nonlinear function of the time interval of the interferometric pair. The random noise may cause a maximum error of about 4mm in the measured settlement when using the 315-day interferogram. The corresponding error for the 35-day pair is about 3mm and this is possibly higher than the possible ground settlement within the period. Therefore, only the 315-day interferogram will be studied further.

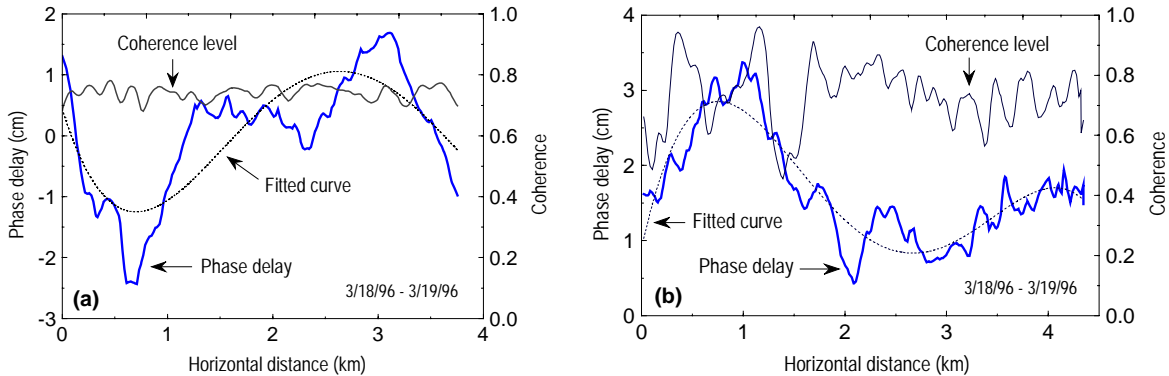


Figure 3: Profiles of atmospheric phase delays and coherence extracted from the one-day interferogram, (a) along line AB and (b) along line CD (see Plate 1).

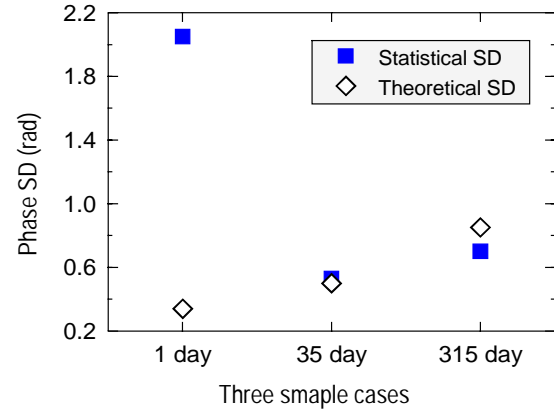


Figure 2: Comparison between statistical and theoretical phase SD for the area of the excavated Chek Lap Kok island.

5. SETTLEMENT MAP AND VALIDATION

5.1 InSAR-levelling comparison over the airport area

We compare in this section the settlement results computed from the 315-day interferogram with levelling measurements at the 28 benchmarks shown in Plate 1.

The interferometric phase values were converted into height changes by means of equations (1) and (2) on a pixel-by-pixel basis. Plate 4 shows the resulting settlement map in the HK80 Grid System with a resolution of $20\text{ m} \times 20\text{ m}$. The subsidence ranges from -50 to 0 mm across the area over the nearly one-year period, while nearly no subsidence is visible throughout the two excavated islands (Plate 1 and 4).

To monitor the stability of the airport platform, a first-order-levelling network has been established and repeatedly surveyed at a frequency of 2-4 times per year by the Airport Authority. As the acquisition time of the InSAR data is different from that for the levelling surveys, interpolation is made to calculate the height changes for the time span corresponding to the SAR data.

Comparing InSAR to levelling measurements at the 28 benchmarks, the mean difference is -3.5 mm and the rms difference is 6.9 mm. Figure 4 gives a scatter plot of subsidence values from the two types of measurements. The results show a correlation of 0.892 , a slope of 1.170

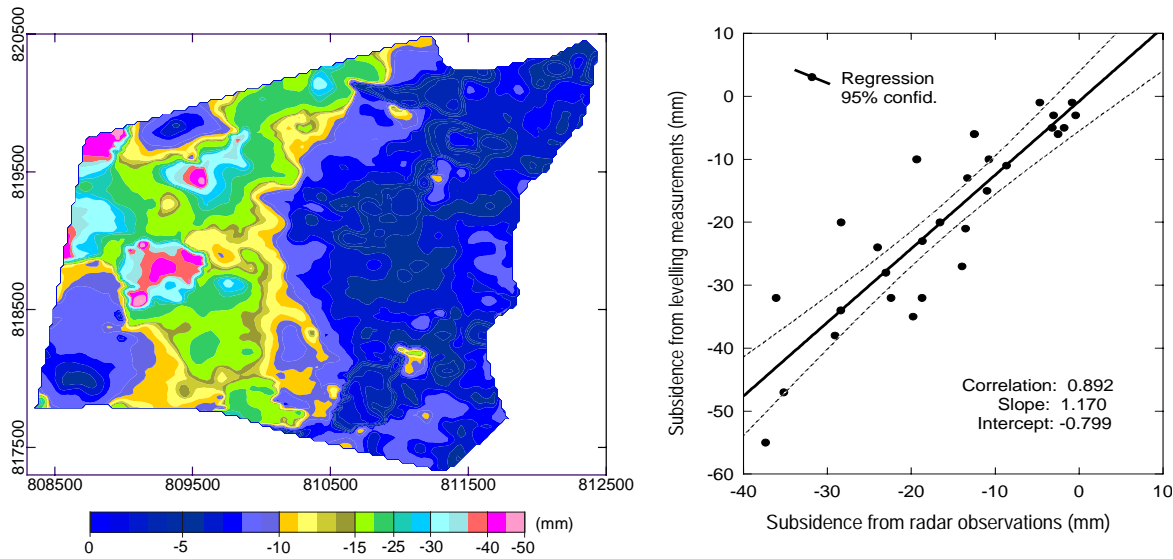


Plate 4: Settlement map from the 315-day interferogram as shown in Plate 3(c).

and intercept of -0.799 in a fitted straight line. The band at the 95% confidence level was given between the dashed lines. Excellent agreement (within 2-3 mm) exists for points in and near the stable areas while divergence (about 10 mm) (points 4, 9, 15, 17 and 20) appears in the reclaimed area.

Figure 4: Scatter plot of the InSAR and levelling subsidence measurements at the 28 benchmarks.

5.2 Settlement over the area of Fairview Park

Fairview Park is a residential area of about 2km² (Figure 1b and Figure 5(a)). The area was reclaimed over 10 years ago. We conducted similar tests as those for the airport as introduced earlier. Good coherence (up to 0.65 on average) was maintained in the area for all the interferometric combinations as those introduced for the airport, even for the pair with an interval of nearly 3 years. This is considered mainly due to the special shapes and finishing of the roofs (see photo in Figure 5). Figure 5(b) shows a 3D-settlement map derived from the SAR image pair acquired on Mar. 19, 1996 and Dec. 29, 1998. The results obtained show that the area has been settling between 1996 and 1999. Although no independent information is available to confirm the interferometric results, the series of settlement maps from other pairs

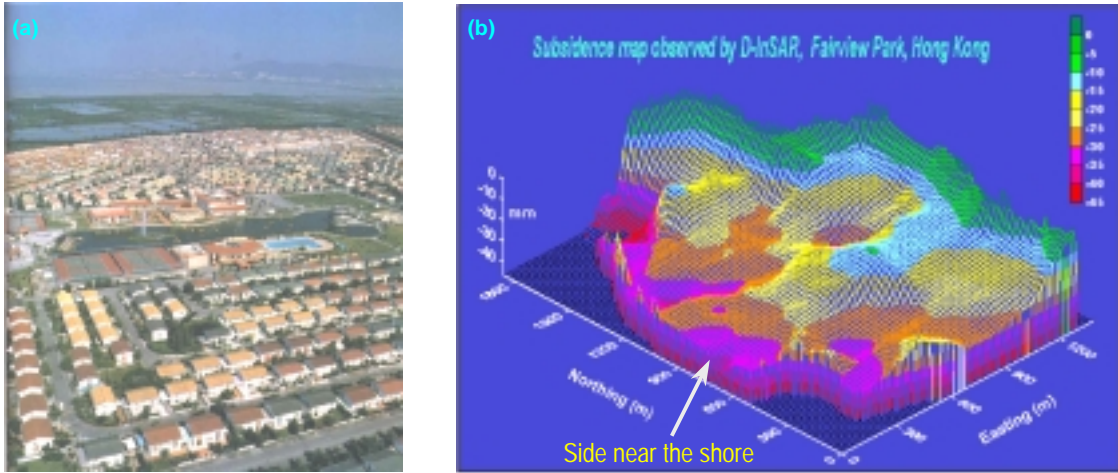


Figure 5: (a) photo of part of Fairview Park, (b) 3D-settlement map near 3 years across the Fairview Park area.

(not shown here) are quite consistent with each other. It is very interesting to note that the subsidence (about 40mm) on the side near the sea is much larger than that (about 0mm) on the side far from the sea, and that the gradual variations across the area are clear (Figure 5(b)).

6. CONCLUSIONS

- The short wavelength (e.g., C band) InSAR has been proven to be a powerful technology to study ground settlement after land reclamations.
- Radar coherence over the tested areas remained high, since the areas were largely covered by man-made surface and structures so that the surface reflective characteristics do not change much with time.
- The 315-day interferogram for the airport area reveals varying magnitudes of settlement (up to 50mm) between Dec. 1998 and Nov. 1999, due mainly to the compression of soils beneath the seabed and the creep of the fill materials. The original outlines of the excavated islands can clearly be identified on the interferogram. The results agree well with levelling measurements. The interferometric measurements over the area of Fairview Park indicate up to 40mm of settlement over a nearly three-year period.

- Since Hong Kong is in the tropical region, the variation in tropospheric water vapour content can cause at times significant phase delays that could seriously contaminate InSAR measurements. For example, the one-day interferogram over the airport shows up to 4cm LOS range changes caused by atmospheric variations.

ACKNOWLEDGEMENTS

The research is partly supported by a grant from the Faculty of Construction and Land Use of the Hong Kong Polytechnic University under the scheme of Cross-Departmental Collaborations. The first author is grateful to the Hong Kong Polytechnic University for the Postgraduate Research Scholarship provided.

REFERENCES

- Bawden, W.G., Thatcher, W., Stein, R.S., Hudnut, K.W., and Peltzer, G., 2001, Tectonic contraction across Los Angeles after removal of groundwater pumping effects. *Nature*, Vol. 412, 812-815
- Chen, Y.Q., Zhang, G.B., Ding, X.L. and Li, Z.L., 2000, Monitoring earth surface deformations with InSAR technology: principle and some critical issues. *Journal of Geospatial Engineering*, Vol.2, 3-21
- Ding, X.L., Ren, D.Y., Montgomery, B., and Swindells, C., 2000, Automatic monitoring of slope deformations using geotechnical instruments. *Journal of Surveying Engineering*, Vol. 126, 57-68
- Fruneau, B., and Sarti, F., 2000, Detection of ground subsidence in the city of Paris using radar interferometry: isolation of deformation from atmospheric artifacts using correlation. *Geophysical Research Letters*, Vol.27, 3981-3984
- Gabriel, A.K., Goldstein, R.M. and Zebker, H.A., 1989, Mapping small elevation changes over large areas: differential radar interferometry. *Journal of Geophysical Research*, Vol.94, 9183-9191
- Galloway, D.L., Hudnut, K.W., and Ingebritsen, S.E. et al., 1998, Detection of aquifer system compaction and land subsidence using interferometric synthetic aperture radar, Antelope Valley, Mojave Desert, California. *Water Resources Research*, Vol.34, 2573-2585
- Goldstein, R.M., Zebker, H.A. and Werner C.L., 1988, Satellite radar interferometry: two-dimensional phase unwrapping. *Radio Science*, Vol.23, 713-720.
- Liu, G.X., Ding, X.L., Chen, Y.Q., Li, Z.L. and Li, Z.W., 2001a, Settlement field of Chek Lap Kok Airport, Hong Kong, detected by satellite synthetic aperture radar interferometry. *Chinese Science Bulletin*, Vol.46, 1778-1782
- Liu, G.X., Ding, X.L., Chen, Y.Q., Li, Z.L., and Li, Z.W., 2001b, The pre- and co-Seismic ground displacements of the 1999 Chi-Chi earthquake from ERS-SAR interferometry, Proceedings of the 4th APSG Workshop (APSG 2001), 14-18 May, Shanghai. Also to appear in *Chinese Journal of Geophysics*.
- Massonnet, D., Rossi, M., Carmona, C. et al, 1993, The displacement field of the Landers earthquake mapped by radar interferometry. *Nature*, Vol.364, 138-142

- Massonnet, D., Holzer, T. and Vadon, H., 1997, Land Subsidence caused by the East Mesa geothermal field, California, observed using SAR interferometry. *Geophysical Research Letters*, Vol.24, 901-904
- Massonnet, D. and Feigl, K., 1998, Radar interferometry and its application to changes in the Earth's surface. *Reviews of Geophysics*, Vol.36, 441-500
- Plant, G.W., Covil, C.S. and Hughes, R.A., 1998, Site Preparation for the New Hong Kong International Airport. 50-80, *Thomas Telford Publishing Ltd, London*
- Rosen, P.A., Hensley, S., Zebker, H.A., Webb, F.H. and Fielding, E.J., 1996, Surface deformation and coherence measurements of Kilauea Volcano, Hawaii, from SIR-C radar interferometry. *Journal of Geophysical Research*. Vol.101, 23109-23125
- Zebker, H.A. and Goldstein, R.M., 1986, Topographic mapping from interferometric synthetic aperture radar observations. *Journal of Geophysical Research*, Vol.91, 4993-4999
- Zebker, H.A., Rosen, P.A., Goldstein, R.M., Gabriel, A. and Werner, C.L., 1994a, On the derivation of coseismic displacement fields using differential radar interferometry: the Landers earthquake. *Journal of Geophysical Research*, Vol.99, 19617-19634
- Zebker, H.A., Werner, C.L., Rosen, P.A. and Hensley, S., 1994b, Accuracy of topographic maps derived from ERS-1 interferometric radar. *IEEE Transactions on Geoscience and Remote Sensing*, Vol.32, 823-836
- Zebker, H.A., Rosen, P.A. and Hensley, S., 1997, Atmospheric effects in interferometric synthetic aperture radar surface deformation and topographic maps. *Journal of Geophysical Research*, Vol.102, 7547-7563

BIOGRAPHICAL NOTES

G.X. Liu and **Z.W. Li** are Ph.D. students. **Prof. Y.Q. Chen** is the Head of Department and Chair Professor. **Dr. X.L. Ding** and **Dr. Z.L. Li** are Associate Professors.